# Pressure Response in Supersonic Wind-Tunnel Pressure Instrumentation*

ARNOLD L. DUCOFFE†
*University of Michigan, Ann Arbor, Michigan*

(Received January 13, 1953)

In the development of high-speed aircraft, rockets, missles, etc., wind-tunnel pressure measurements at supersonic velocities are necessary to determine certain aerodynamic characteristics. Because of the lack of knowledge concerning the proper choice of parameters in the design of pressure instrumentation, the response time has been known to exceed the running time in the case of the intermittent tunnel. Pressure systems consisting of an orifice, a capillary tube, a length of connecting tubing, and a pressure-sensitive element connected in series are analyzed. The time required for the pressure in the pressure-sensitive element to reach within 1 percent of the equilibrium pressure is defined as the response time of the system. Experiments are conducted to determine the effect of the various geometric and dynamic parameters on the response time. Analytical solutions of the flow equations by numerical integration are carried out for the special case of a length of capillary tubing connected to the pressure-sensitive element for three different inside diameters.

The data indicate that the response time can be maintained within acceptable limits for present-day supersonic wind-tunnel installations by proper choice of the geometric and dynamic parameters. The agreement between theory and experiment, being quite satisfactory for the special case solved analytically, indicated that the approximations in the derived flow equations are justified.

## NOTATION

$a$ = tube radius
$d$ = inside diameter of model tubing
$d_c$ = inside diameter of connecting tubing
$d_0$ = orifice diameter
$f$ = total number of gas molecules
$i$ = subscript to indicate spatial stations
$j$ = subscript to indicate time stations
$k$ = constant ($=RT$)
$l$ = length of model tubing
$l_c$ = length of connecting tubing
$m'$ = rate of mass flow
$p$ = pressure
$p_c$ = capsule pressure
$p_{c0}$ = initial pressure in capsule reservoir at zero time
$p_m$ = mean pressure
$p_R$ = reservoir pressure
$r$ = radius
$t$ = time
$\bar{t}$ = nondimensional time
$u$ = velocity component in the direction of the $x$ axis
$u_0$ = velocity at the boundary in slip flow
$x$ = spatial position in tubing
$z$ = coordinate
$A$ = constant
$B$ = constant
$F$ = slip-flow parameter
$F_T$ = viscous shearing force
$F_T'$ = viscous shearing force in slip flow
$H$ = slip-flow parameter
$P$ = nondimensional pressure
$R$ = gas constant
$T$ = absolute temperature
$V$ = volume of capsule reservoir
$X$ = nondimensional spatial coordinate
$\epsilon$ = coefficient of external friction
$\lambda_m$ = mean free path of molecules
$\mu$ = coefficient of viscosity
$\mu_E$ = effective viscosity coefficient
$\rho$ = mass density
$\rho_1$ = density at 1 micron of pressure
$\tau$ = response time
$\mathbb{S}$ = coefficient of slip

## FLOW EQUATIONS

THREE general types of flow can exist in capillary tubes; namely, continuum flow, slip flow,[1] and free-molecule flow.[2] The type of flow which one might encounter is dependent on the medium used, the magnitude of the mean pressure in the tubing, and the radius of the tubing. For the case at hand, the magnitudes of the mean pressure and the radii of the tubing are chosen to represent typical supersonic wind-tunnel pressure measurements. The resulting flow is then found to be almost exclusively in the realm of a continuum flow.

The derivation of the equation of motion is based on the assumption of a continuous medium, constant-area tubing, and a fully developed flow over the entire length of the tubing. The change of state of the flow is assumed to be described by an isothermal process; and, by the introduction of the unsteady, compressible continuity equation, the quasi-steady, viscous, com-

* This research was conducted at the University of Michigan in partial fulfillment of the requirements for the degree of Doctor of Philosophy. Thanks are due Dr. A. M. Kuethe and Dr. L. L. Rauch for their invaluable guidance and encouragement in all phases of the work.

† Associate Professor of Aeronautical Engineering and Research Associate, Georgia State Engineering Experiment Station.

[1] Brown, Dinards, Cheng, and Sherwood, J. Appl. Phys. 17, 802 (1946).

[2] S. A. Scharf and R. R. Cyr, "Time constants for vacuum gauge systems," University of California Report No. H E—150-42 (1948).

pressible equation of motion is developed. The boundary equations are developed assuming a finite reservoir, in which the changes of state take place isothermally, at one end of the tubing and an infinite reservoir (pressure constant) at the other end of the tubing. The initial distribution of pressure $p(x)$ is assumed to be a step function with the pressure discontinuity located immediately before the infinite reservoir. Schematically the idealized model of a typical supersonic wind-tunnel pressure system is shown in Fig. 1. The resulting nonlinear, partial differential equation of motion and boundary equation are solved by numerical step-by-step integrations for three different conditions in which the capillary tube diameter as well as the reservoir pressure are varied.

Starting with the Hagen-Poiseuille law[3] for fully developed flow (and assuming the flow is fully developed over the entire length of the tubing), the rate of mass flow can be written as

$$m' = -\frac{\pi\rho a^4}{8\mu}\frac{\partial p}{\partial x}, \tag{1}$$

where $m'$ is the rate of mass flow, $\rho$ is the mass density, $a$ is the radius of the tubing, $\mu$ is the coefficient of viscosity, $p$ is the pressure, and $x$ is the spatial coordinate.

The incompressible flow equation (1) is modified to include the effects of compressibility by means of the isothermal equation of state,

$$p = k\rho, \tag{2}$$

where $k=(RT)$ is a constant, $R$ being the universal gas constant, and $T$ the absolute temperature. Substituting Eq. (2) into Eq. (1) we obtain

$$m' = -\frac{\pi}{8\mu k}a^4 p\frac{\partial p}{\partial x}. \tag{3}$$

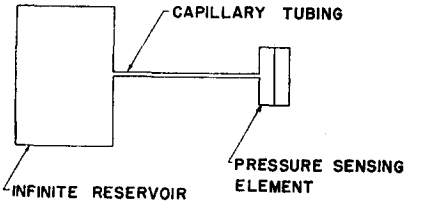


FIG. 1. Idealized model of pressure system.

Assuming one-dimensional unsteady flow the continuity equation may be written as

$$\frac{\partial}{\partial x}(\rho u) = -\frac{\partial \rho}{\partial t}, \tag{4}$$

where $t$ is time. If we now take an incremental length ($\Delta x$) of tubing (Fig. 2) and substitute the rate of mass flow given by Eq. (3) into Eq. (4), we obtain in the limit as $\Delta x \to 0$

$$\frac{\partial p}{\partial t} = \frac{a^2}{8\mu}\frac{\partial}{\partial x}\left(p\frac{\partial p}{\partial x}\right). \tag{5}$$

The boundary conditions are derived for the physical system shown in Fig. 3. Because of the large ratio of surface area to chamber volume in typical pressure capsules (in this case, approximately 320:1), the change of state in the capsule reservoir is assumed to be isothermal. The boundary condition for the flow out of the capsule ($x=0$) is obtained by equating the rate of mass flow in the tubing [Eq. (3)] to the rate of change

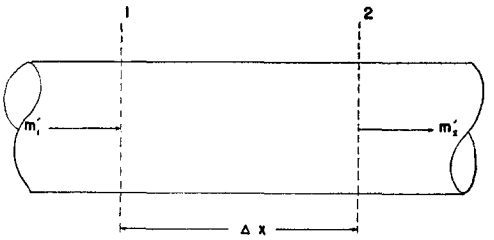


FIG. 2.

of mass in the capsule. This results in

$$\left.\frac{\partial p}{\partial t}\right]_{x=0} = \left.\frac{\pi a^4}{8V\mu}p\frac{\partial p}{\partial x}\right]_{x=0}, \tag{6}$$

where $V$ is the capsule volume (assumed constant since calculations[4] indicate only a few percent change on account of diaphragm deflection).

The boundary condition at $x=l$ simulates the condition at a model orifice in a steady wind-tunnel flow, that is, constant pressure. Thus

$$\left.p\right]_{x=l} = \text{constant}. \tag{7}$$

The initial condition in the pressure is taken as a step function and is given by

$$\begin{aligned} p(0, x) &= A, \\ p(0, l) &= B, \end{aligned} \tag{8}$$

where $A$ and $B$ are constants.

Equation (5) represents the differential equation of motion for the one-dimensional, quasi-steady, developed, viscous, compressible flow in capillary tubing. The equation characterizes a nonlinear diffusion process and has the same form as the heat equation with the thermal conductivity being proportional to the tem-

[3] A. M. Kuethe and J. D. Schetzer, *Foundations of Aerodynamics* (John Wiley and Sons, Inc., New York, 1950), p. 222.

[4] S. Timoshenko, *Theory of Plates and Shells* (McGraw-Hill Book Company, Inc., New York, 1940), p. 60.

perature. Solutions[5,6] of Eq. (5) have been presented for initial conditions and boundary conditions not applicable in the present case.

### Nondimensionalized Equations of Motion and Boundary Equations

The equation of motion and boundary equations are nondimensionalized in order to study the important nondimensional parameters which govern the flow. On the basis of previous experimental information, the characteristic pressure, length, and time are taken as the reservoir pressure $p_R$, length of capillary tubing $l$, and response time of the system $\tau$, respectively. The resulting nondimensional equations are

Equation of motion:

$$\frac{\partial P}{\partial \dot{t}}=-\frac{1}{8}\left(\frac{a^2}{l^2}\frac{p_R\tau}{\mu}\right)\left[\left(\frac{\partial P}{\partial X}\right)^2+P\frac{\partial^2 P}{\partial X^2}\right]. \tag{9}$$

Boundary conditions:

at $X=0$

$$\frac{\partial P}{\partial \dot{t}}=-\frac{\pi}{8}\left(\frac{a^2}{l^2}\frac{p_R\tau}{\mu}\right)\left(\frac{la^2}{V}\right)P\frac{\partial P}{\partial X}, \tag{10}$$

at $X=1$:

$$P=1, \tag{11}$$

where $P$, $X$, $\dot{t}$ are the nondimensional pressure, spatial coordinate, and time, respectively. From Eqs. (9) and (10) it is seen that two nondimensional parameters appear. The parameter $[(a^2/l^2)(p_R\tau/\mu)]$ is termed a dynamic similarity parameter and is found in both equations, whereas the geometric similarity parameter $(la^2/V)$ is found only in Eq. (10).

### Analytical Solutions

Attempts to solve the differential equation of motion and boundary equations failed and resort was made to a numerical solution in the form of step-by-step integrations. The equations are approximated by finite differences. Initially the derivatives were approximated by straight line sequents but, after several steps were computed using this method, it was found that the term involving

$$\left[\left(\frac{\partial P}{\partial X}\right)^2+P\frac{\partial^2 P}{\partial X^2}\right]$$

contains two terms of almost equal magnitude but of opposite sign. This results in the subtraction of two large numbers whose difference is relatively much smaller in magnitude. In order to minimize the errors, the curve of $P$ *vs* $X$ was approximated by parabolas.[7,8] The resulting equations in difference form are given as

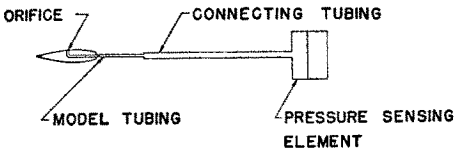


FIG. 3. Schematic diagram of a typical pressure system.

Equation of motion:

$$P_{i,j+1}=P_{i,j}+\frac{1}{8}\left(\frac{a^2}{l^2}\frac{p_R}{\mu}\right)\times\left[\left|\left(\frac{2P_{i+2}+P_{i+1}-P_{i-1}-2P_{i-2}}{10}\right)_j\right|^2+\frac{P_{i,j}}{7}(2P_{i+2}-P_{i+1}-2P_i-P_{i-1}+2P_{i-2})_j\right]\frac{\Delta t}{\Delta X^2}. \tag{12}$$

Boundary equations:

at $X=0$

$$P_{0,j+1}=P_{0,j}+\frac{\pi}{8}\left(\frac{a^2}{l^2}\frac{p_R}{\mu}\right)\left(\frac{a^2l}{V}\right)\times P_{0,j}(P_{0+1}-P_0)_j\ddagger\frac{\Delta t}{\Delta X}, \tag{13}$$

at $X=1$:

$$P_{1,j}=\text{constant}=1, \tag{14}$$

where the subscripts "$i$" and "$j$" denote spatial stations and time stations, respectively.

Three numerical solutions were calculated for the idealized system shown in Fig. 1. The idealized system is used because the discontinuities in the tubing area (Fig. 3) at the junctures of the orifice and connecting tubing with the capillary tubing cannot be handled readily in the step-by-step integrations. As a result three cases of the idealized system were computed numerically and compared with experiment in order to determine whether the derived equation of motion and boundary equations approximated the actual flow process in the tubing. The orifice and connecting tube can be considered as end effects; that is, the orifice could be replaced by an additional length of capillary tubing and the connecting tube by an additional volume in the pressure sensing unit. These effects are handled conveniently by experiment rather than as additional complications in the theoretical equations. The initial steps in the numerical integration were made with very small time increments (0.000001 sec) in order that the

[5] Arthur S. Iberall, J. Research Natl. Bur. Standards 45, RP 2115 (1950).

[6] J. M. Kendall, "Time lags due to compressible-Poiseuille flow resistance in pressure-measuring systems," NOLM 10677 (1950).

[7] F. A. Willers, *Practical Analysis* (Dover Publications, New York, 1948), p. 310.

[8] J. B. Scarborough, *Numerical Mathematical Analysis* (Johns Hopkins University Press, Baltimore, Maryland, 1950), p. 132.

‡ The derivative $\partial P/\partial X$, at $X=0$, was computed by two methods. A plot of $P$ *vs* $X$ was made and $\partial P/\partial X$ at $X=0$ measured graphically. Also a plot of $\partial P/\partial X$ *vs* $X$ was made and faired into $X=0$. Both methods proved successful; thus, one method served as a check on the other.

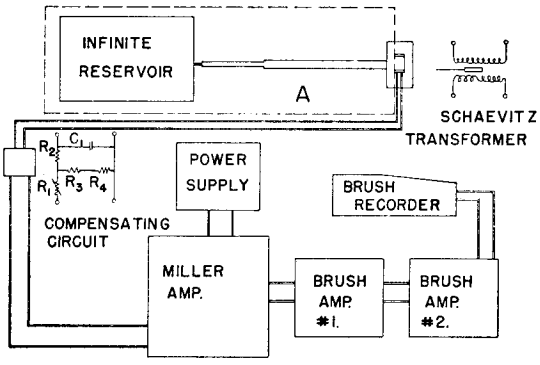


FIG. 4. Block diagram of experimental apparatus.

step function in the pressure (initial condition) could be approximated by derivatives resulting in negligible errors.

## DESCRIPTION OF APPARATUS

The test apparatus was designed to simulate typical supersonic wind-tunnel pressure instrumentation systems. A block diagram of the complete system is shown in Fig. 4.

The pressure capsule, developed at the supersonic wind tunnel at the University of Michigan, is shown in Fig. 5. This instrument, having a negligible time lag, was ideally suited for this work. The capsule is machined from 24 ST bar stock and has a diaphragm approximately 0.025 inch thick and 3 inches in diameter. Calibrations of the capsule showed that the deflection of the diaphragm at its center is linear with load (pressure). The motion of the diaphragm is transduced by a differential transformer whose linear range was more than adequate for the range of diaphragm deflections encountered in these tests. Model or probe tubing used in typical supersonic tunnel tests was simulated by stainless-steel hypodermic needle tubing. The connecting tubing, that is, the tubing ordinarily used to join the model tubing and a differential mercury manometer, was simulated by copper tubing since rubber and plastic tubing were found to be too porous at low absolute pressures. Figures 6 and 7 show the simulated orifice assemblies. The pressure reservoir, analogous to the test section (constant pressure) in a supersonic tunnel, consisted of two tanks manifolded together with a combined capacity of $22\frac{1}{2}$ cubic feet. With this capacity runs could be made at reservoir pressures of 5-mm Hg absolute with less than $\frac{1}{2}$ percent change in reservoir pressure under the most extreme conditions in these experiments. The reservoir pressures were maintained by means of a vacuum pump and a Wallace and Terrian dial-type pressure gauge.

The electronic recording equipment shown in Fig. 4 consists of a Miller amplifier and power supply, linear differential transformer in the pressure capsule, a capsule compensating circuit, two Brush dc amplifiers, and a Brush recorder. The power supply provides the operating potentials for the tubes in the Miller amplifier and also provides a 2-kc carrier voltage for excitation of the bridge circuit formed by the Miller amplifier and the capsule compensating circuit. The compensating circuit serves three basic purposes:

(1) Resistance $R_1$ and condenser $C_1$ provide the proper phase balance between the differential transformer and the carrier voltage originating in the power supply.

(2) Resistance $R_2$ serves as a current-limiting resistor in order to protect the transformer from excess current.

(3) Resistances $R_3$ and $R_4$ provide two external bridge arms which combine with the two arms built into the Miller amplifier to form a bridge circuit.

The function of the Miller amplifier is threefold: (a) the ac signal from the pressure capsule is first ac amplified; (b) the amplified ac signal is then rectified and then the detector, being phase sensitive, gives the signal a sign (+ or −), depending on the motion of the diaphragm being positive or negative; (c) the dc output signal is then dc amplified. The output signal from the Miller amplifier, being $\pm\frac{1}{4}$ volt, is then amplified by two

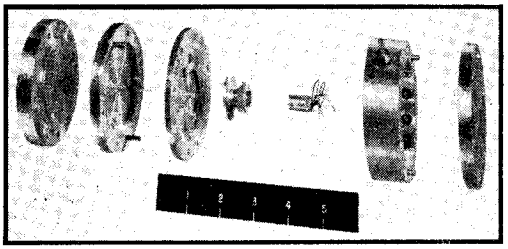

FIG. 5. Exploded view of pressure capsule.

dc amplifiers since $\pm 15$ volts is required to drive the Brush recorder pen full scale from the center of the paper. In addition the two Brush amplifiers are necessary for additional sensitivity.

## EXPERIMENTAL PROCEDURE

### Tests Conducted for Correlation with Theory

In order to compare the three numerical solutions with experiment, three tests were made using the idealized system shown in Fig. 1. Since the Brush recorder paper is only 40 mm wide, the desired sensitivity over the entire absolute pressure range (e.g. atmospheric to 20-mm Hg) could not be maintained. In order to circumvent this difficulty the following procedure was used: For the initial run the gain of the Brush amplifiers was set so that the pressure change (atmospheric to 20-mm Hg) was traced out on approximately the full width of the paper (curve *a*, Fig. 8). Atmospheric pressure was then reintroduced into the lines and capsule, and the gain increased so that a pressure of 100-mm Hg absolute in the capsule would correspond to the top line on the recorder paper. This resulted in

the pen being off scale against the mechanical stops until the capsule pressure approached 100 mm, after which the pen traced out the remainder of the run until the equilibrium pressure of 20-mm Hg was reached (curve *b*, Fig. 8). The same procedure was repeated for succeeding runs, using full-scale deflection for top line pressures of 50- and 21-mm Hg absolute (curves *c* and *d*, Fig. 8). A continuous curve of capsule pressure *vs* time was obtained by plotting the data from the four individual runs.

### Tests Conducted to Show Effects of Important Parameters

In typical pressure instrumentation in supersonic wind-tunnel testing (Fig. 3), certain parameters are considered as being of prime importance in determining the response time characteristics of the system. These parameters are listed as:

(a) orifice diameter $d_0$;
(b) inside diameter of model tubing $d$;
(c) length of model tubing $l$;

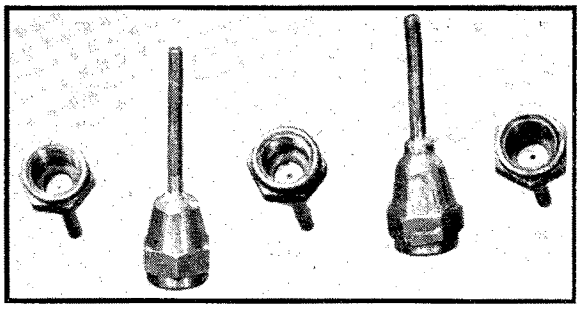

FIG. 6. Orifice assemblies.

(d) inside diameter of connecting tubing $d_c$;
(e) length of connecting tubing $l_c$;
(f) local pressure at model orifice (reservoir pressure) $p_R$;
(g) initial pressure in capsule reservoir and instrument lines at time=0 $p_{c0}$; and
(h) volume of pressure-sensing element $V$.

Since the time lag in any system will depend on the capacity of the pressure-sensing element, it is obvious that the volume of this unit should be designed with a minimum capacity. For this reason the pressure capsule used in these tests was designed with a volume which is small compared to the combined volumes of the capillary and connecting tube. The parameter (*h*) was not varied but was held constant at its value of 0.106 cubic inch. The parameters (a)–(g) were chosen each with a specific range corresponding to the values used in present-day intermittent tunnels.

#### (*a*) *Orifice Diameter* $d_0$

No criteria seem to be available in the literature as to the optimum size of an orifice in supersonic flow

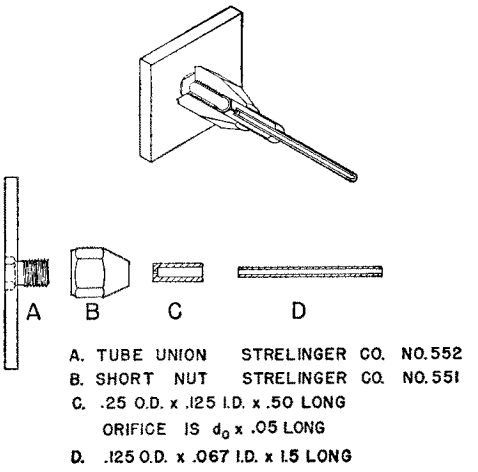


FIG. 7. Details of orifice assembly.

research. Too large an orifice can cause disturbances to the flow in the neighborhood of the body, whereas too small an orifice can result in a large response time due to restriction of the mass flow in or out of the lines. The orifice length is usually quite small. A representative value of 0.05 inch was used. Five orifice diameters (0.045, 0.035, 0.025, 0.020, and 0.015 inch) were selected.

#### (*b*) *Model Tubing Diameter d*

In most supersonic tunnels the model sizes are restricted by relatively small test sections. The model support through which the tubing is carried must also be as small as possible to minimize interference effects. The size of the model tubing (especially for the case where a large number of pressure orifices are required) is therefore limited. Five inside diameters were chosen; namely, 0.063, 0.054, 0.042, 0.031, and 0.025 inch. The tests conducted to show model tube diameter effect were made with length as a parameter.

#### (*c*) *Model Tubing Length l*

The model tubing lengths (2, 4, 6, 8, and 10 feet) were selected to cover the range for installations in operation at the present time and also in anticipation of the requirements of much larger supersonic tunnels which inevitably will be built. The tests to show length

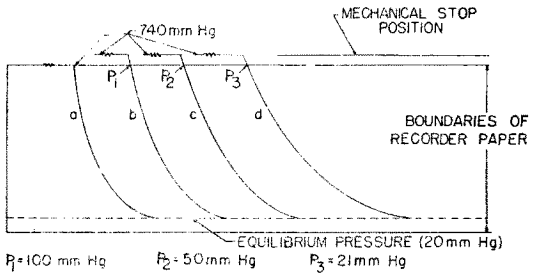


FIG. 8. Recorder traces used to obtain desired sensitivity over complete range of capsule pressures.

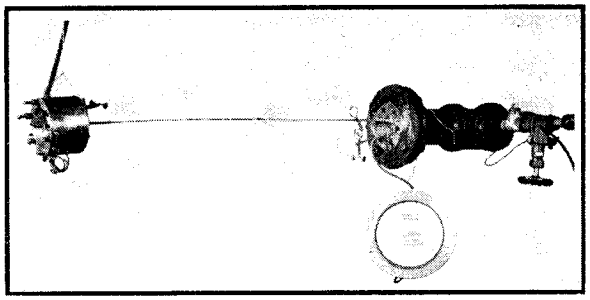

FIG. 9. Orientation of capsule, pressure line, and orifice test setup.

effect were run using each of the five values of $d$ for each tube length and the remaining parameters held constant as described in the tests for the evaluation of the model tube diameter effect.

### (d) *Connecting Tube Diameter $d_c$ and Length $l_c$*

In most installations the pressure-sensing unit must of necessity be located external to the tunnel. For this reason a length of connecting tubing is required. In order to investigate the parameters $d_c$ and $l_c$, three values of $d_c$= (0.067, 0.083, and 0.125 inch) and $l_c$= (0, 60, and 120 inches) were tested.

### (e) *Reservoir Pressure $p_R$*

Reservoir pressures, corresponding to the static pressures measured on a model, were chosen with the following values 50-, 30-, 20-, 15-, 10-, and 5-mm Hg absolute. For blowdown tunnels using atmospheric pressure as a stagnation condition, these pressures correspond to test-section Mach numbers ranging for 2.42 to 4 for isentropic flow. Each of the five model tube diameters were tested with each reservoir pressure. The other parameters ($d_0$=0.025-, $l$=24-, $l_c$=60-, $d_c$=0.067-, and $p_{c0}$=740-mm Hg) were held constant throughout this series of experiments.

### (f) *Initial Line and Capsule Reservoir Pressure $p_{c0}$*

The effect of changing the initial capsule reservoir and line pressure will be to reduce the mass of air which

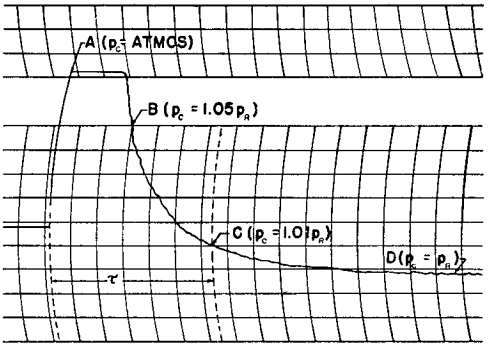


FIG. 10. Typical brush recorder trace showing $p_c$ *vs* time ($1.05p_R \leq p_c = p_R$).

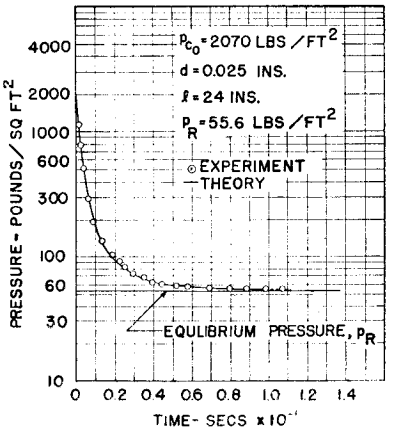


FIG. 11. Comparison of theoretical and experimental pressure variation in the capsule reservoir.

must be evacuated before the system reaches equilibrium. In the previous tests the pressure in the capsule reservoir and lead lines was set at atmospheric pressure merely for convenience in running the experiments.

The experimental setup for the condition wherein

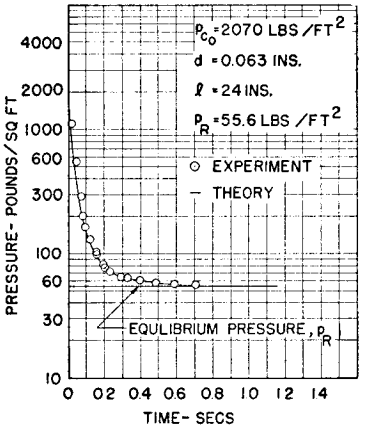


FIG. 12. Comparison of theoretical and experimental pressure variation in the capsule reservoir.

no connecting tube is used is shown in Fig. 9. The pinchcock at the left is used to introduce any desired pressure into the capsule reservoir and lines. The upper pinchcock at the right simulates a quick-opening valve for exhausting the air from the capsule to the reservoir;

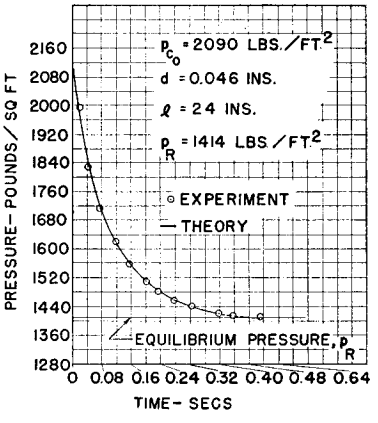


FIG. 13. Comparison of theoretical and experimental pressure variation in the capsule reservoir.

while the lower pinchcock serves as a means to adjust the reservoir pressure in the $22\frac{1}{2}$-cubic foot tank.

## REDUCTION OF DATA

As shown in Fig. 10 the capsule pressure approaches the equilibrium (reservoir) pressure asymptotically. The response time is defined as the time required for the capsule pressure to reach within one percent of the reservoir pressure. In order to obtain sufficient sensitivity the top line of the Brush recorder paper corresponds to a capsule pressure of $p_c = 1.05 p_R$. The starting point is designated by $A$, the point where $p_c = 1.01 p_R$ by $C$, and the equilibrium value ($p_c = p_R$) by $D$. The response time ($\tau$) is then the distance between $A$ and $C$, measured as shown in Fig. 10, divided by the paper speed (mm/sec).

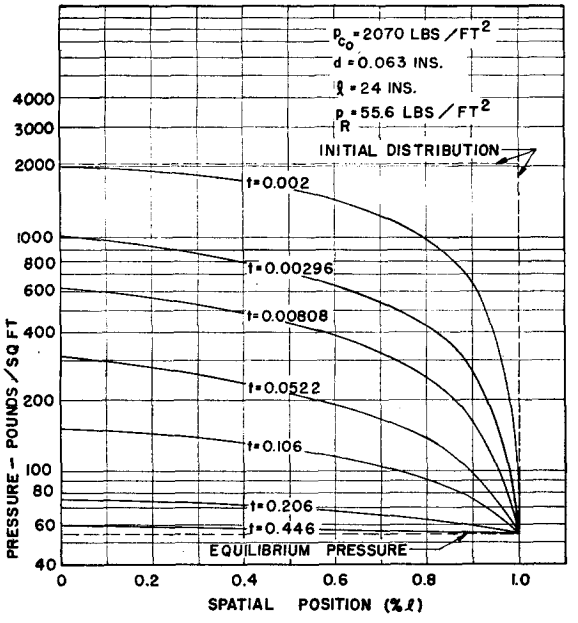


FIG. 14. Spatial pressure distribution.

## RESULTS

The variation of capsule pressure as a function of time for the three cases computed numerically is shown in Figs. 11 through 13 as solid lines, while the experimental results are indicated on the same plots by circled points. The step-by-step integrations were carried to the point where $p_c = 1.025 p_R$; hence, the broken line from $p_c = 1.025 p_R$ to $p_c = 1.01 p_R$. The agreement between theory and experiment is quite satisfactory, indicating that the approximations in the derived flow equations and boundary conditions are justified. Spatial pressure distributions in the tubing obtained in the step-by-step integration procedure are presented in Figs. 14 through 16 in which only a few of the actually computed steps are shown. The curves give a qualitative description of the manner in which the spatial pressure distribution changes from that of a step function at zero time to essentially the condition of equilibrium.

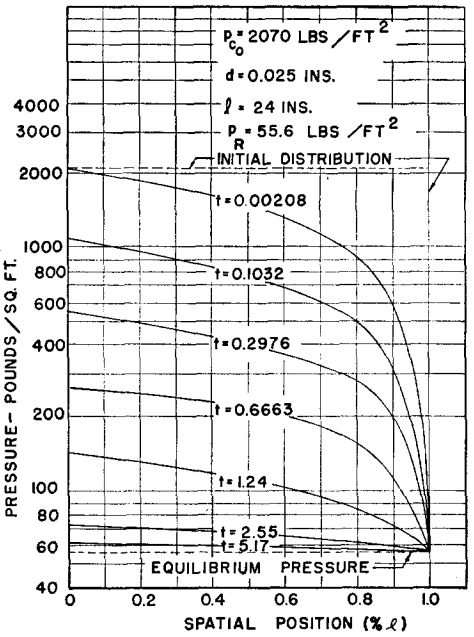


FIG. 15. Spatial pressure distribution.

The effect of each parameter on the response time, $\tau$, is presented as a series of graphs in Figs. 17 through 23.

### (a) Orifice Effect

The orifice effect is shown in Fig. 17 by a plot of response time *vs* orifice diameter, $d_0$, with tube diameter, $d$, as a parameter. The results indicate that the orifice size does not appreciably effect the response time until the ratio of tube diameter to orifice diameter approaches 2.5. As this value is exceeded the response time as compared with the response time for no orifice starts to increase rapidly as is evidenced by the curve for $d = 0.063$ in. The effect of decreased orifice size is

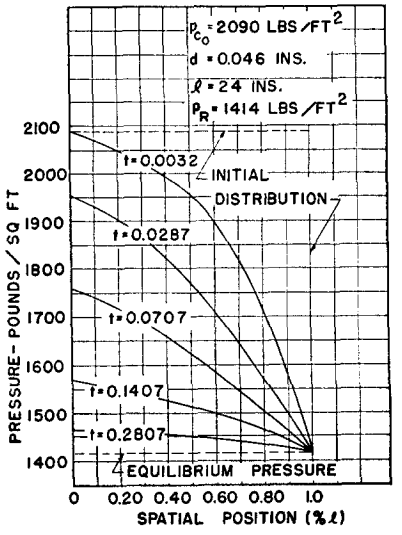


FIG. 16. Spatial pressure distribution.

analyzed as a restriction of the flow of air through the system and thus as an increase in the response time.

### (b) Diameter Effect

The effect of changing the model tube diameter is shown by a plot of response time *vs* tube diameter with length as a parameter in Fig. 18. From the graph it is seen that the diameter of the tubing is very critical if the response time is to be minimized. A change in diameter has essentially two effects: (1) the capacity of the system is altered, and (2) the rate of mass flow through the system is changed. The effect of changing the capacity of a typical system as a result of change in the tube diameter is almost negligible (as will be shown later). Hence, the increase in response time for decreased tube diameters is attributed primarily to the restriction of the mass flow through the system.

### (c) Length Effect

The length effect is derived from a crossplot of Fig. 18 and is shown in Fig. 19. Since the slopes of the curve increase with decreased diameter, the effect of length is seen to be more pronounced for the smaller diameters.

### (d) Connecting-Tube Diameter and Length Effects

The results of varying the dimensions of the connecting tube are shown in Fig. 20. The connecting-tube effect is twofold; (1) the connecting tubing contributes the major portion of the capacity of the system, and (2) it offers resistance to the flow through the system. Referring to Fig. 20 for the case of $d=0.063$ in., one notes that the curve for $d_c=0.067$ has a larger response time than the curve for $d_c=0.083$ for the two lengths

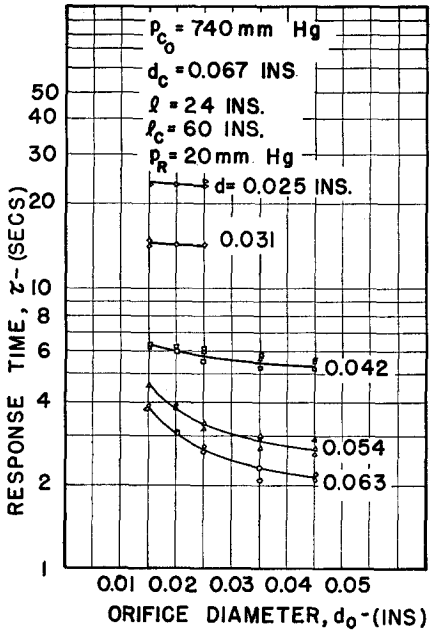


FIG. 17. Orifice effect, $d_0$.

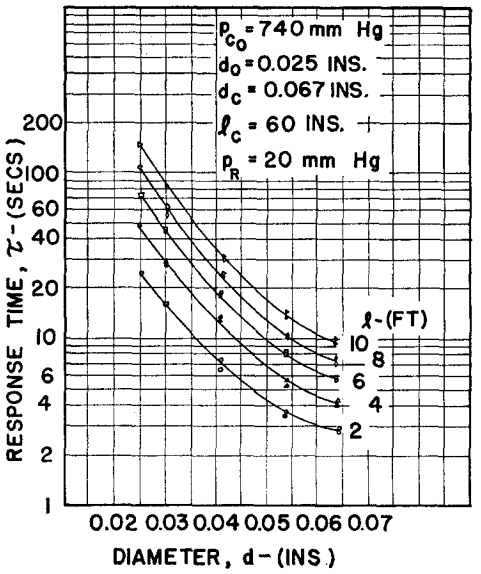


FIG. 18. Diameter effect, $d$.

$l_c=60$ and 120 in. This is explained by the fact that the $d_c=0.067$ tube has almost the same diameter as the model tube (0.063 in.). Thus, in this case the connecting tube not only increases the capacity of the system, but also gives rise to large viscous forces, thus restricting the flow in the same manner as the capillary tubing.

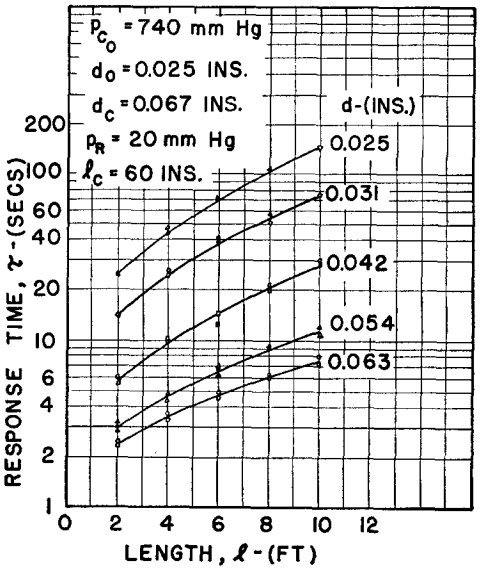


FIG. 19. Length effect, $l$.

The other connecting-tube diameters ($d_c=0.083$ and 0.125 in.), being considerably larger than the model tubing, influence the response time primarily by the resultant increased capacity of the system. For the other extreme in model-tube diameter (0.025 in.), the effect of increasing the diameter, $d_c$, is an increased capacity and an expected increase in response time.

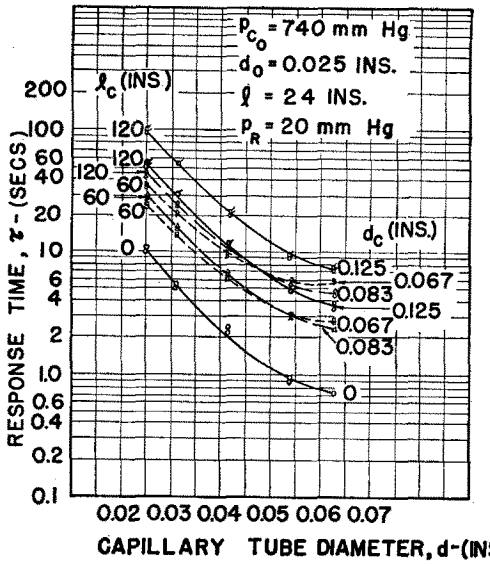


FIG. 20. Connecting tube effect, $d_c$ and $l_c$.

### (e) Reservoir Pressure Effect

The effect of changing the reservoir pressure is presented in Fig. 21. The curves indicate that the absolute value of the pressure has a large effect on the response time. If we examine the equation of motion

$$\partial p/\partial t = K[(\partial p/\partial x)^2 + p(\partial^2 p/\partial x^2)]$$

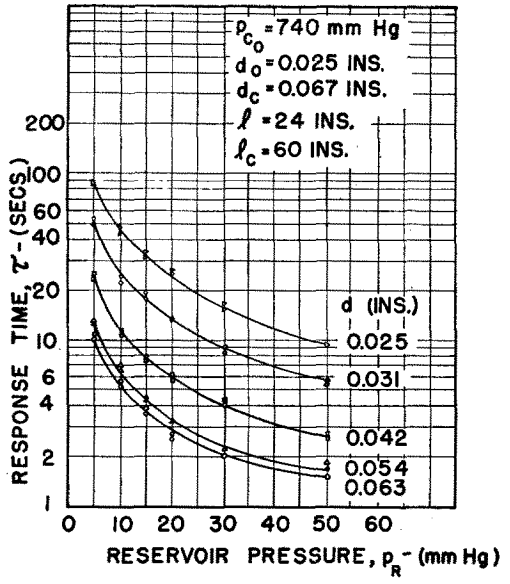


FIG. 21. Reservoir pressure effect, $p_R$.

and boundary equation at $x=0$

$$\partial p/\partial t]_{x=0} = K_1 p(\partial p/\partial x)]_{x=0},$$

we find that the nonlinearities in the equations indicate that, if the pressure is halved everywhere, the response time is increased by a factor of 2. Referring to Fig. 21, we find that, if we start with an initial line and capsule

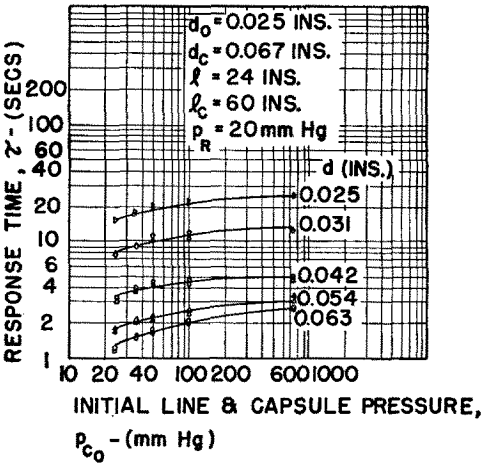


FIG. 22. Initial line and capsule pressure effect, $p_{c_0}$, $p_R$ = 20-mm Hg.

pressure of 740-mm Hg and a reservoir pressure of 20-mm Hg and then reduce the reservoir pressure to 10-mm Hg, the response time is approximately doubled. It will be shown later that halving the instrument line and capsule reservoir pressure has almost negligible effect on the response time. As a result, it is evident that the particular nonlinear character of the differential equation of motion is substantiated by experiment. We may also see from the equation of motion that the term $(\partial p/\partial x)^2$ is always positive and for flow out of the lines the term $[p(\partial^2 p/\partial x^2)]$ will be negative. Thus, for a given spatial distribution of pressure, $p(x)$, at any instant the amount the pressure decreases at each spatial station for a given time increment will depend on the absolute value of the pressure.

### (f) Initial Line and Capsule Pressure Effect

The effect of evacuating the line and capsule reservoir pressures to a value approaching the constant reservoir pressure is shown in Figs. 22 and 23 for reservoir pres-

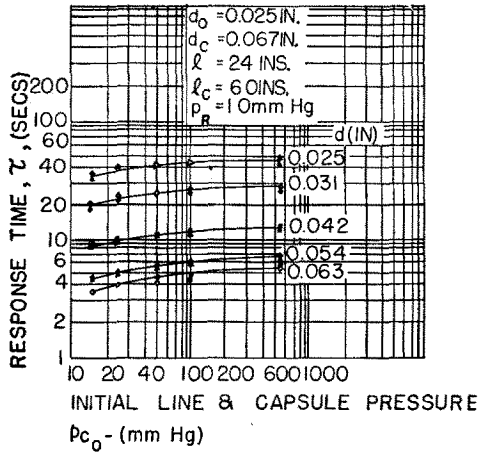


FIG. 23. Initial line and capsule pressure effect, $p_{c_0}$, $p_R$ = 10-mm Hg.

sures of 20- and 10-mm Hg absolute, respectively. As is shown in the graphs, the advantages of pumping down are quite small unless the capsule and line pressures approach the reservoir pressure within 1-mm Hg or less. For the case of a pressure model where 20–30 leads might be used the amount of time gained during any run would be considerably less than the time required to evacuate each line to the predicted pressure at each orifice.

### *Experimental Errors*

The reservoir pressures in the range $5 \leq p_R \leq 20$ (mm Hg) were set within $\pm 0.1$-mm Hg. For the range $20 \leq p_R \leq 100$ (mm Hg) the error in gauge reading was $\pm 0.20$-mm Hg.

The lag of the Brush recorder pen under a step-function change in voltage was measured to be 0.01 sec for full-scale pen defection. Since the capsule pressure changes in an exponential manner, the pen lag will be considerably smaller, and is estimated to be of the order of 0.003 sec for the most rapid pressure changes encountered in the experiments. The time required to open the quick-opening valve (pinchcock) could not be determined readily. However, the results of check runs indicate that this time lag was so small that it could not be detected. In any event, for each value of $\tau$ for a particular experimental setup at least two check runs were made and $\tau$ computed from an arithmetical average of at least three readings.

## CONCLUSIONS

### Limitations of Theoretical Analysis

On the basis of the satisfactory agreement between theory and experiment, we may conclude that the initial assumptions of quasi-steady developed laminar flow with isothermal changes of state closely approximate the flow conditions in the tubing. However, several limitations must be imposed on the theoretical development, since the theory is applicable over only a specified range of the parameters chosen for investigation.

(a) Over the chosen range of tubing diameter, the condition of isothermal change of state is applicable; however, as the tubing diameter is increased the thermodynamic process involved becomes polytropic and finally approaches the condition of an isentropic process. No attempt has been made to analyze the transition states between the isothermal and isentropic processes, since most supersonic pressure systems fall well within the range of diameters investigated.

(b) The assumption of continuum flow is applicable until the reservoir pressure (or model-surface pressure) drops below 20-mm Hg absolute (see Appendix). For lower absolute pressures, the equation of motion for the flow must be modified to account for the violation of the no-slip condition at the boundaries of the tubing. The slip condition is incorporated into the equation of motion by the introduction of an experimentally derived effective coefficient of viscosity and is defined by the ratio of the normally computed coefficient of viscosity to a slip-flow correction factor. Free-molecule flow conditions are probably never approached in supersonic flow research (see Appendix).

(c) The assumption of fully developed laminar flow is violated for two reasons. First, flow in tubing becomes fully developed at a position many diameters downstream from the entrance of the tube; and second, for the large pressure drop over the initial part of the experiments the flow may be turbulent.

Further limitations on the theory are the end effect where the air exits from the tubing into the reservoir and the expansion effects where the tubing is coupled to the pressure reservoir and the capsule.

Since the effects previously described cannot be handled conveniently in the theoretical development, discrepancies between the theory and the experimental data will exist.

### Limitations of Experiments

(a) The experimental setup was designed to reproduce actual pressure systems with the exception of 90° bends inside the pressure models, which are necessary in order to take the model leads through the sting or support. These bends are usually fairly gradual (large radii of curvature) and the effects are considered to be negligible.

(b) In the experimental procedure the pressure drop across the tubing was chosen so that air flowed out of the capsule reservoir at all times. Thus, no information is available on the response time for air flowing in the opposite direction. The technique is justified on the basis of the differential equation of motion, wherein the nonlinearity predicts that the response time is a function of the absolute pressure of the system. Thus, for a given reservoir pressure we see that line pressures greater than the equilibrium pressure are more advantageous on a response time basis than line pressures below the equilibrium value. However, for small values of the equilibrium pressures (below 20-mm Hg absolute) some advantage is to be gained by initial line pressures less than 20-mm Hg absolute because of the condition of slip flow at the boundaries.

(c) The experimental results apply only for pressure-sensing elements having an infinitesimal mechanical response time. For systems employing manometers, the dynamic and viscous effects of the fluid columns will in some cases increase the response time considerably.

### Criteria for Minimum Response Time

The following criteria in the choice of suitable parameters are presented for the design of pressure instrumentation with minimum response times:

(a) The orifice diameter should not be less than one-half the model-tubing diameter, with slight advantage

to be gained as the orifice diameter approaches the tubing diameter.

(b) The model tubing should be made as short as possible, incorporating the largest inside diameter that is feasible.

(c) Connecting tubing should be short, with the inside diameter lying between $1\frac{1}{4}$ to $1\frac{1}{2}$ times the inside diameter of the model tubing.

(d) The capacity of the sensing-unit reservoir should be minimized.

(e) The advantage of pumping the initial reservoir and line pressure to a value close to the model-surface pressure is quite small unless the initial pressure approaches the equilibrium pressure to within 1-mm Hg.

## APPENDIX

### Criteria for Slip Flow and Free-Molecule Flow

*Slip Flow*

The equation of motion for steady, isothermal, developed flow is derived from Eq. (5) by setting $\partial p/\partial t=0$ and is given by

$$(\partial p/\partial x)^2+p(\partial^2 p/\partial x^2)=0, \tag{15}$$

the boundary conditions being

$$\begin{aligned} p&=p_0 \quad \text{at} \quad x=0 \\ p&=p_1 \quad \text{at} \quad x=l. \end{aligned} \tag{16}$$

The rate of mass flow, $m'$,[6] is then given by

$$m'=(\pi a^4/16\mu kl)(p_0^2-p_1^2), \tag{17}$$

where $k$ is the proportionality constant in the isothermal equation of state. The derivation of Eq. (17) is based on the assumption that the coefficient of viscosity, $\mu$, is a constant, i.e., proportional to the temperature which is constant in an isothermal change of state, and that the condition of no slip at the walls of the tube is valid. The assumption of a constant coefficient of viscosity at moderate and high pressures is predicted by kinetic theory.[9] However, the failure of Eq. (17) at low pressures is explained by the failure of the no-slip condition at the walls rather than on the basis of a variable viscosity.

Under the conditions of small pressures, the condition of no slip at the wall is violated,[1,9,10] since the coefficient of viscosity now becomes a function of the pressure. The derivation of Poiseuille's law is modified in that the velocity at the wall is taken as $u_0$ instead of 0 when the mean free path of the molecules is comparable with the tube radius. The resulting tangential force, $F_T$, on the wall, which for the condition of no slip is written as

$$F_T=\mu(du/dy)\big]_{y=0}, \tag{18}$$

is now modified and assumed proportional to $u_0$ and to the surface area $A$,

$$F_T'=\epsilon u_0 A, \tag{19}$$

where the constant $\epsilon$ is termed the coefficient of external friction. Balancing the viscous and pressure forces over an incremental length of tubing $dl$, we have

$$-\pi a^2 dp=F_T'=2\pi a\epsilon u_0 dl, \tag{20}$$

which gives

$$u_0=-(a/2\epsilon)(dp/dl). \tag{21}$$

In order to determine the average velocity for the condition of slip flow at the walls, we start with an analogous expression[9] for $u_0$ given by

$$u_0=\mathcal{S}(du/dz)\big]_{z=0}=-\mathcal{S}(du/dr)\big]_{r=0}, \tag{22}$$

where $\mathcal{S}$ is a constant called the coefficient of slip and is defined by the relation $\mathcal{S}=\mu/\epsilon$. The Poiseuille equation[3] for the velocity in a continuum flow, given by

$$u=(r^2/4\mu)(dp/dx)+c\log_e r+c_1, \tag{23}$$

is now employed with modified boundary conditions given by

$$\begin{aligned} u&=u_0 \quad \text{at} \quad r=a, \\ du/dr&=0 \quad \text{at} \quad r=0. \end{aligned} \tag{24}$$

Substituting these boundary conditions into Eq. (23) and employing relationship [Eq. (22)], we have

$$u=\frac{r^2}{4\mu}\frac{dp}{dx}+\frac{a^2}{4\mu}\frac{dp}{dx}-\frac{\mathcal{S}a}{2\mu}\frac{dp}{dx}, \tag{25}$$

or more simply

$$u=(1/4\mu)(r^2-a^2-2\mathcal{S}a)(dp/dx). \tag{26}$$

The mass flowing past any cross section of the tube per second is

$$m'=\frac{p}{k}\int_0^a 2\pi r u dr,$$

or

$$m'=-\frac{\pi}{8}\frac{a^4}{k\mu}\left(1+4\frac{\mathcal{S}}{a}\right)p\frac{dp}{dx}. \tag{27}$$

The integrated form of Eq. (27) is identical to that of Eq. (17), except for the additive constant $(4\mathcal{S}/a)$. Thus, we may write

$$m'=\frac{\pi a^4}{16\mu l}(p_0^2-p_1^2)\left(1+\frac{4\mathcal{S}}{a}\right). \tag{28}$$

Maxwell suggests that a fraction $f$ of the gas molecules striking the walls of the tubing would be reflected diffusely; that is, the molecules would suffer a complete loss of their initial average tangential velocity. The fraction $1-f$ of the gas molecules would be reflected specularly; that is, with no change in their tangential velocity. According to the predictions of kinetic theory,[9]

[9] E. H. Kennard, *Kinetic Theory of Gases* (McGraw-Hill Book Company, Inc., New York, 1938), p. 292.

[10] S. Dushman, *Scientific Foundations of Vacuum Technique* (John Wiley and Sons, Inc., New York, 1949), p. 84.

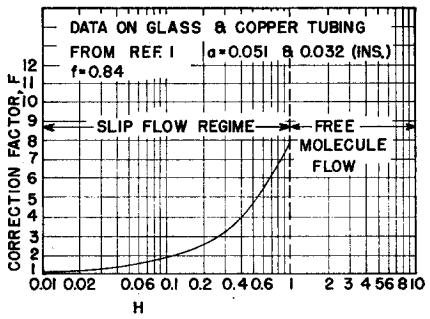


FIG. 24. Slip-flow correction factor.

the coefficient of slip can be written as

$$\mathcal{S}=[(2/f)-1]\lambda_m, \tag{29}$$

where $\lambda_m$ is the mean free path of the molecules at the mean pressure in the tubing. Thus, we may write for Eq. (28)

$$m'=\frac{\pi a^4}{16\mu l}(p_0^2-p_1^2)\left[1+4\left(\frac{2}{f}-1\right)\frac{\lambda_m}{a}\right]. \tag{30}$$

From kinetic theory and Maxwell's distribution of molecular velocities the mean free path[1] is given by

$$\lambda_m=(\pi/2\rho_1)^{\frac{1}{2}}(\mu/p_m), \tag{31}$$

where $\rho_1$ is the gas density at 0.001-mm Hg and $p_m$ is the mean pressure of the flow. Substituting Eq. (31) into Eq. (30), we have

$$m'=\frac{\pi a^4}{16\mu l}(p_0^2-p_1^2)\left[1+4\left(\frac{\pi}{2}\right)^{\frac{1}{2}}\left(\frac{2}{f}-1\right)H\right], \tag{32}$$

where $H$ represents the term $[\mu/p_m a(\rho_1)^{\frac{1}{2}}]$. Examination of Eq. (32) indicates that the slip-flow equation is essentially the Poiseuille equation (17) multiplied by a correction factor which assumes importance as the ratio, $(\lambda_m/a)$, of the mean free path to the tube radius increases and also as $f$ becomes small (smooth walls). Experimental data[1] for the determination of the factor

$$1\left[+4\left(\frac{\pi}{2}\right)^{\frac{1}{2}}\left(\frac{2}{f}-1\right)H\right],$$

which is denoted by $F$ for flow in copper capillary tubing, is presented in Fig. 24. The tests were run using air as the flow medium, with tube radii of 0.0512 and 0.0313 inch. The effect of slip is accounted for by defining an effective viscosity which is given by the relation

$$\mu_E=\mu/F. \tag{33}$$

The factor $H$ can be simplified for ease in interpreting Fig. 24 by substitution of appropriate values; it reduces to

$$H=4.10/p_m a, \tag{34}$$

where $p_m$ is the mean pressure $(p_0+p_1)/2$ in microns of mercury (1 micron=0.001-mm Hg) and $a$ is the tube radius in cm. In the theoretical calculations for the 0.025-inch inside-diameter tubing and a reservoir pressure of 20-mm Hg, $H$ is found to be

$$H=\frac{4.10}{20\,000\times 0.0125\times 2.54}=0.00647.$$

Referring to Fig. 24, the factor $F$ is found to be approximately 1, so that no correction for slip is necessary. However, for a reservoir pressure of 5-mm Hg, the value of $H$ would be increased to 0.0259 and from Fig. 24 the value of $F$ is seen to be 1.22, so that slip-flow corrections are necessary.

On the basis of the above calculations it can be seen that slip-flow corrections are not necessary for the numerical solutions, since the smallest reservoir pressure investigated was 20-mm Hg. However, in those experiments where the reservoir pressure was set at 5-, 10-, and 15-mm Hg, slip flow probably occurs in the smaller-diameter capillary tubes.

### *Free-Molecule Flow*

At very low pressures the internal friction of the fluid becomes very small because the mean free path of the molecules becomes large compared to the radius of the tubing. Under these conditions the collisions between molecules are very infrequent and may be neglected. This assumption[2] is valid if the mean pressure in microns ($10^{-3}$ mm Hg absolute) is less than the reciprocal of the tubing diameter in inches,

$$p_m<1/2a. \tag{35}$$

For the case of supersonic wind-tunnel testing, where the mean pressure might be as low as 5000 microns and the tubing inside diameter may be as small as 0.020 inch, it can readily be seen that free-molecule flow is not approached. That is,

$$p_m(=5000)\gg 1/2a(=50).$$